Electronic structure of the charge-density-wave compound $Er_5Ir_4Si_{10}$

2006 J. Phys.: Condens. Matter 18 5773

(http://iopscience.iop.org/0953-8984/18/24/017)

INSTITUTE OF PHYSICS PUBLISHING JOURNAL OF PHYSICS: CONDENSED MATTER

J. Phys.: Condens. Matter **18** (2006) 5773–5782 doi:10.1088/0953-8984/18/24/017

Electronic structure of the charge-density-wave compound $Er_5Ir_4Si_{10}$

F Bondino[1,6], E Magnano[1], E Carleschi[1], M Zangrando[1], F Galli[2], J A Mydosh[3] and F Parmigiani[1,4,5]

[1] Laboratorio Nazionale TASC INFM-CNR, Basovizza-Trieste, Italy
[2] Kamerlingh Onnes Laboratorium, Universiteit Leiden, Postbus 9504, 2300 RA Leiden, The Netherlands
[3] II. Physikalisches Institut, Universität zu Köln, D-50937 Köln, Germany
[4] Dipartimento di Fisica, Università degli Studi di Trieste, Trieste, Italy
[5] Sincrotrone Trieste S.C.p.A., Basovizza-Trieste, Italy

E-mail: bondino@tasc.infm.it

Received 20 February 2006
Published 2 June 2006
Online at stacks.iop.org/JPhysCM/18/5773

Abstract

Photoemission and x-ray absorption measurements have been performed on $Er_5Ir_4Si_{10}$, a compound that exhibits an incommensurate charge-density-wave formation below 155 K. The resonant photoemission and x-ray absorption measurements performed across the Er N_{54} and Er M_5 edge identify the Er 4f multiplet lines, the 4f occupancy and the character of the states close to the Fermi edge.

1. Introduction

Ternary rare-earth (R) iridium silicides $R_5Ir_4Si_{10}$ have attracted considerable attention due to the coexistence of charge density wave (CDW) and long-range magnetic ordering or superconductivity at low temperature [1, 2]. A paradigm here is $Er_5Ir_4Si_{10}$, an intermetallic compound that crystallizes in a three-dimensional tetragonal structure (space group: $P4/mbm$) and displays anomalies at 155 and 55 K in all transport, structural and thermodynamical properties [3, 4]. For example, the resistivity (ρ) curve exhibits a metallic character in the normal state above 155 K (T_{CDW}), while below this temperature a different metallic (partially gapped) state with reduced conductivity is present. In $Er_5Ir_4Si_{10}$, the anisotropy ratio in the resistivity along the two crystallographic directions, defined as ρ_a/ρ_c, is $\sim$2.4 [3], much smaller than in canonical CDW systems. The family of R_5T_4Si/Ge_{10} (where T = transition metal) showing CDWs all have small and comparable anisotropy (see [5, 6]).

X-ray diffraction measurements prove that these anomalies are due to a strongly coupled commensurate (at 55 K) and incommensurate (at 155 K) CDW formation [3, 5]. In spite of the three-dimensional (3D) structure of this crystal, the chain-like structure of Er atoms along

[6] Author to whom any correspondence should be addressed.

the c axis may form a quasi-one-dimensional electron band that can be fundamental for the appearance of the CDW.

In addition, $Er_5Ir_4Si_{10}$ displays an antiferromagnetic (AFM) phase transition at 2.8 K, making this compound a unique example of a magnetic system exhibiting a CDW [7]. The observation of a resistivity depression by the application of a magnetic field leading to a negative magnetoresistance at low temperatures [4] suggests a possible interplay between CDW and magnetism [4]. This interplay is further supported by the observation that the localized Er magnetic moments are aligned along the c axis, where the periodic lattice distortion associated with the CDW also takes place [7].

Similar complex behaviour has been found in $Lu_5Ir_4Si_{10}$, which displays a strongly coupled first-order CDW formation below 83 K and a coexisting superconducting state below 3.9 K [8, 9, 6]. $Lu_5Ir_4Si_{10}$ has the same stoichiometry and tetragonal structure as $Er_5Ir_4Si_{10}$, but shorter lattice parameters [2] and no magnetism due to the lanthanide contraction and the filled 4f shell.

The partially filled 4f shell of the Er atoms in $Er_5Ir_4Si_{10}$ gives rise to large localized magnetic moments of 9.6 μ_B [4]. The magnetic mechanism leading to the long-range AFM coupling at low temperature in this system has been described as an indirect Ruderman–Kittel–Kasuya–Yosida (RKKY) exchange interaction [10] between the spins of the localized 4f electrons interacting via spin polarization of conduction electrons [7]. The same conduction electrons that play an essential role in the magnetism as the mediators of magnetic interactions between the 4f states are also responsible for the CDW formation and putative Fermi surface instability.

When a CDW emerges, a nesting of the Fermi surface and the opening of a partial or total (pseudo) gap at the Fermi level (E_F) is expected to take place. In fact, in $Er_5Ir_4Si_{10}$, below 155 K the conductivity is reduced along the c axis and a reduction of the density of states (DOS) at E_F due to the formation of a partial gap was suggested to take place from the muon relaxation rate measurements [11]. Presently, optical conductivity experiments are underway to probe the gap opening and its anisotropy directly [12].

Although the structural, electric and magnetic properties of the $Er_5Ir_4Si_{10}$ phases are rather well investigated experimentally, the electronic properties of this system are almost unknown. It is important to have experimental results that can provide benchmarks for electronic structure calculations. It is therefore interesting to investigate the modifications of the valence band (VB) across the CDW transition and the interplay of the lanthanide 4f electrons responsible for the local moment magnetism with the itinerant electrons, which can be involved in the CDW transitions. It is also important to assess the presence and the character of the itinerant electrons in the valence band. Since the 4f states in Er are usually located in a binding energy (BE) range between 4 and 12 eV, the presence of the electrons directly involved in the chemical bonds and in phase transitions (Er 5d, Er 6sp, Si 3spd, Ir 5d) can be evaluated from photoelectron spectroscopy (PES). In particular, the character of these states can be determined by exploiting the elemental selectivity obtained by tuning the photon energy across the absorption edge of a particular atom of the compound.

In this work we have investigated the electronic structure of $Er_5Ir_4Si_{10}$ by means of PES and x-ray absorption spectroscopy (XAS), while resonant photoemission (resPES) has been used to study the partial DOS close to E_F.

2. Experiment

The experiment has been performed on the BACH beamline at Elettra in Trieste [13, 14]. Linear and circular polarized light in the 35–1600 eV range is provided by two APPLE II helical

undulators. The monochromator resolution was set to 0.6 eV in the Er M_{54} photon energy range and 0.1 eV in the Er N_{54} energy range.

The $Er_5Ir_4Si_{10}$ and $Lu_5Ir_4Si_{10}$ single crystals were synthesized in a tri-arc crystal puller using the Czochralski technique. The crystals were fully characterized by x-ray diffraction and electron-probe microanalysis, which proved them to be single phase (secondary phases $<1\%$) and with the correct stoichiometry [3, 9].

The sample surface was cleaved at 300 K at a pressure lower than 3×10^{-10} mbar. In order to keep the sample surface free from contamination during the experiment, the sample was scraped or sputtered using Ar^+ ions. Surface cleanliness was checked continuously by monitoring the O 1s and Si 2p core levels and the VB.

The photoemission measurements were performed using a 150 mm-VSW hemispherical-electron analyser with a 16-channel detector. The absorption spectra were recorded in total electron yield, collecting simultaneously the photocurrent emitted by the sample and the reference current I_0 from the horizontal refocusing mirror of the beamline as a function of the incident photon energy. The XAS data were normalized by the reference I_0 to the absorption edge jump, and the energy scale was always calibrated with valence band photoemission spectra.

3. Results and discussion

3.1. X-ray absorption spectroscopy

In figure 1(a), the Er M_{54} XAS spectrum measured at room temperature (RT) is shown. The experimental spectrum (markers) is compared to the result of multiplet calculation (solid line) performed for a $4f^{11}$ configuration extracted from [15]. Below T_{CDW}, an identical Er M_{54} XAS lineshape is observed (not shown here).

Figure 1(b) displays the Er N_{54} XAS spectrum measured at RT and the result of multiplet calculation performed for a $4f^{11}$ configuration extracted from [16]. The Er N_{54} XAS spectrum obtained below T_{CDW} (not shown here) shows an identical lineshape. The spectrum exhibits several structures preceding the giant absorption, and it is well reproduced by the calculation by Ogasawara and Kotani for an Er^{3+} ion considering 4d4f excitation and the dominant 4d4f4f super-Coster–Kronig decay channel [16].

Since, in the N_{45} edge for heavy lanthanides, the $4f \rightarrow \varepsilon f$ tunnelling, where a continuum electron is emitted with low kinetic energy, is not relevant, the XAS lineshape is insensitive to the environment and is mainly determined by 4f occupancy [16]. The good agreement of the experimental Er M_{54} and N_{54} XAS spectra with the multiplet calculation for a [Xe] $4f^{11}$ ground state [15, 16] (see figure 1) indicates that the 4f electron occupancy is 11 for all Er ions in $Er_5Ir_4Si_{10}$. No variation across the CDW transition is observed in the Er M_{54} and N_{54} XAS spectra, indicating no change in the Er 4f occupancy. The $4f^{11}$ configuration for Er derived from these measurements fully supports the results of the magnetic measurements that found, for $Er_5Ir_4Si_{10}$ single crystals, a magnetic moment consistent with a $4f^{11}$ (Er^{3+}) configuration [4, 7].

3.2. Photoemission spectroscopy

Figure 2 shows the Er 4d core level obtained at RT with $h\nu = 664.9$ eV and a total energy resolution of 0.35 eV. The experimental spectrum is reported, together with the spectrum resulting from a calculation performed for a $4f^{11}$ configuration extracted from [17]. The spectrum exhibiting a complex line distribution is determined by intra-atomic interaction between the 4d core hole and the 4f shell. It is separated by an exchange interaction in a

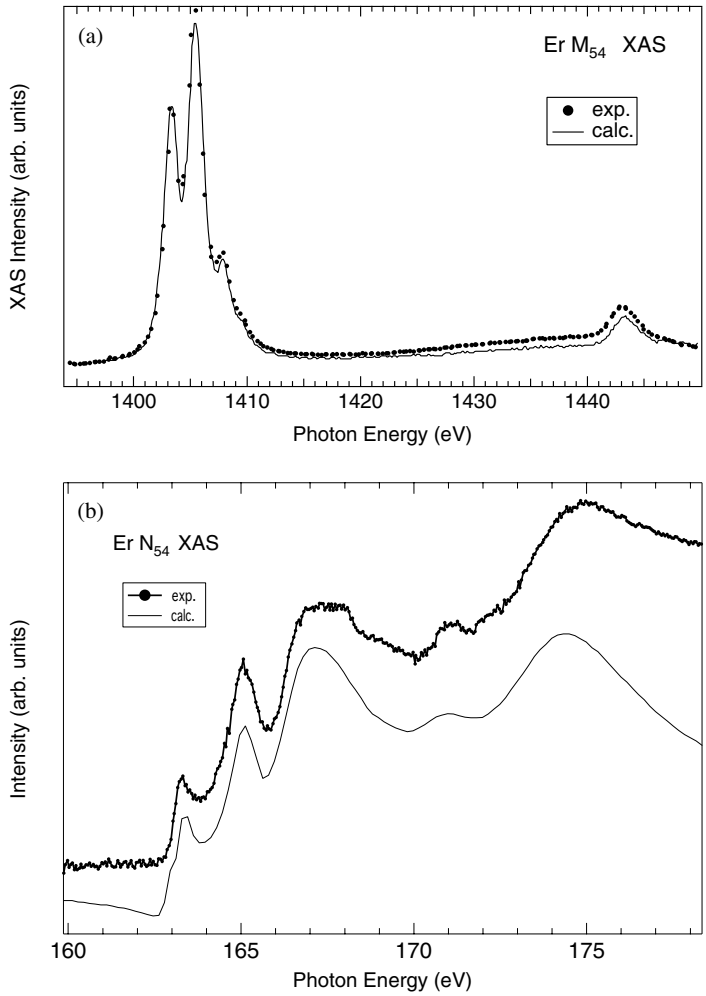

Figure 1. (a) The Er M_{54} XAS spectrum measured at 300 K is compared to the result of multiplet calculation performed for a $4f^{11}$ configuration extracted from reference [15]. (b) The Er N_{54} XAS spectrum measured at 300 K is compared to the result of multiplet calculation performed for a $4f^{11}$ configuration extracted from [16].

low-BE region with narrow peaks and in a higher-BE region with broad lines according to the relative spin orientation of the 4d hole with respect to 4f electrons [17]. The broadening of the lines is determined mainly by the sensitivity to the spin direction of the dominant 4d4f4f super-Coster–Kronig decay process [17]. The multiplet intensity and width in this spectrum is similar to that of metallic Er and Er_3Rh [18, 19], while it is very different from that of Er sesquioxides or pyrosilicates [20, 17, 21]. In particular, Guerfi *et al* have observed how charge transfer affects the Er 4d lineshape and BE: the clear doublet at 167.6 and 169.6 eV observed for metallic Er compounds disappears, replaced by a large peak centred at 170.4 eV in ionic Er compounds. This strong variation makes the Er 4d core level a clear fingerprint of the presence of itinerant electrons in the VB.

Figure 3(b) shows a set of VB spectra measured at RT across the Er M_5 absorption edge at the photon energies corresponding to the open circles in figure 3(a). The main multiplet lines are indicated in the spectra and labelled as A–E. The spectra have been acquired with

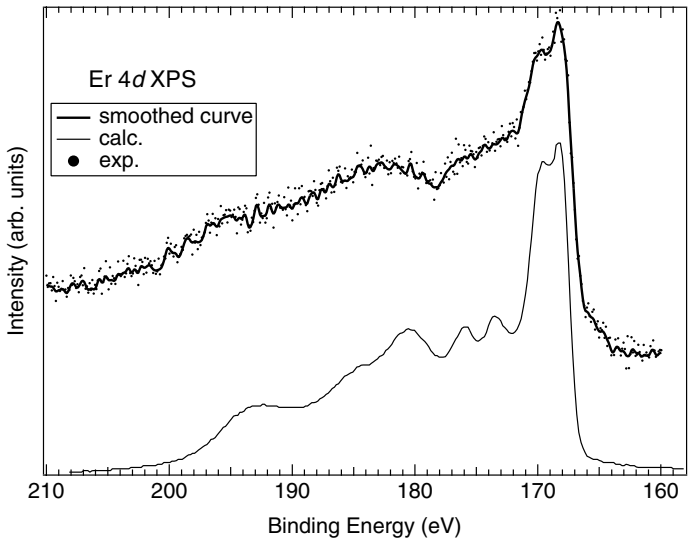

Figure 2. The Er 4d core level obtained at 300 K with a 664.9 eV photon energy and a resolution of 0.35 eV (raw data superimposed on the curve obtained after smoothing) is reported together with the spectrum resulting from a calculation performed for a $4f^{11}$ configuration extracted from [17].

a total resolution of 2.2 eV and normalized to the photon flux. The structures with BEs of around ∼25 and ∼31.5 eV are due to Er 5p emission, and the weak structure around 50 eV is the Er 5s core level, while the doublet with BEs of around 61 and ∼64 eV are the Ir 4f core levels. Using photon energies corresponding to the Er 3d to 4f transition, a giant resonant enhancement of the Er-derived valence states occurs. As the photon energy is varied across the edge, the different multiplets that extend between 5 and 15 eV in the photoemission spectra are enhanced independently. The difference spectrum obtained by subtracting the off-resonance spectrum ($h\nu = 1390.3$ eV) from one of the on-resonance spectra ($h\nu = 1405.3$ eV) is also reported in figure 3(c). In the difference spectrum, a weak spectral weight related to the Er DOS is present in the whole BE range between E_F and the Er 4f multiplets. The same results are obtained at 128 K, below T_{CDW}, in Er M_5 resPES measurements not shown here.

Figure 4 shows the VB spectra normalized to the photon flux and measured across the Er N_{54} absorption edge, on resonance at 167.8 eV and off resonance at 159.8 eV at 115 K, below T_{CDW}. Using photon energies corresponding to the Er 4d to 4f transition, a resonant enhancement of the Er-derived valence states is obtained. The difference spectrum between on and off Er N_{54} resonance spectra is also reported in figure 4. The experimental difference spectrum is compared to the 4f multiplet lines obtained for a $4f^{11}$ configuration from [21]. In the energy region from E_F to 3 eV, the difference spectrum exhibits a weak spectral weight up to E_F. A slightly larger density of Er states is found in a structure with a BE of around 0.2 eV followed by a small dip and broad structures at higher BEs (inset in figure 4). At about 4.5 eV, there is a component not belonging to the $4f^{11}$ lines.

No variations in the VB difference spectrum obtained by subtracting on and off Er N_{54} resonance spectra are observed at 183 K, above the CDW transition with respect to the measurements at 115 K. Also, above T_{CDW} the difference spectrum (not shown here) shows a spectral weight starting from E_F to the beginning of the 4f multiplet lines both in the Er M_5 and in the Er N_5 resPES measurements.

The difference spectrum obtained by subtracting the Er N_{54} off-resonance spectrum from the on-resonance spectrum (see figure 4) identifies the structures originating from the Er partial

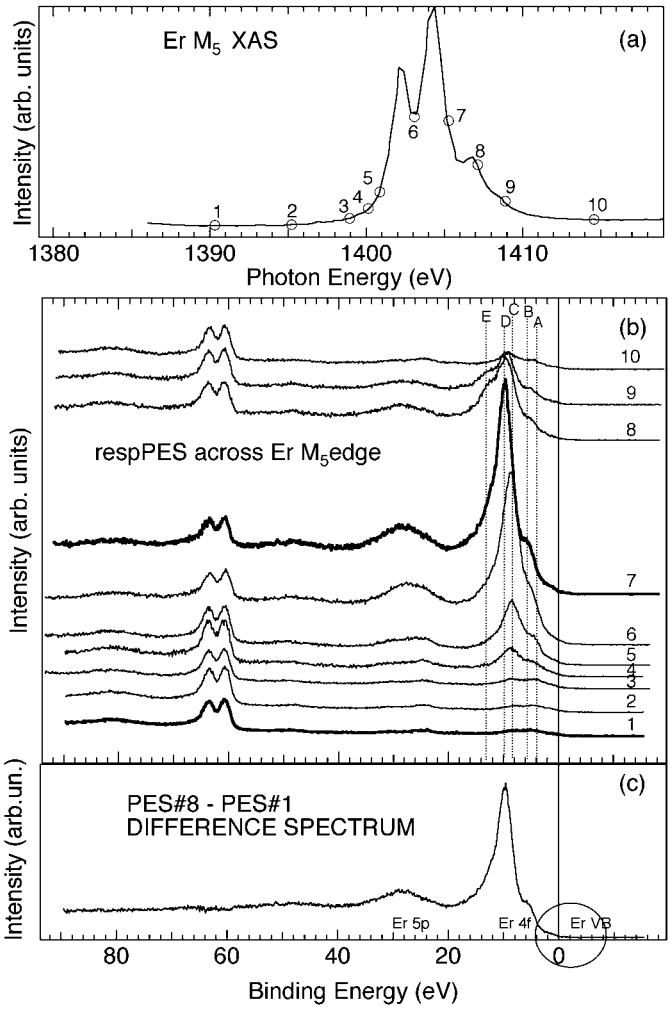

Figure 3. (a) Er M_5 absorption edge, with the photon energies used for the resPES VB measurement indicated as open circles. (b) A set of normalized VB resPES spectra measured at RT across the Er M_5 absorption edge at the photon energies indicated in (a). (c) The difference between the spectra measured at $h\nu = 1405.3$ eV and at $h\nu = 1390.3$ eV.

DOS. In this difference spectrum, the Er 4f multiplet lines, identified from the comparison with calculations, extend over a BE range of ∼10 eV, between 5 and 15 eV. The 4f multiplets are shifted towards a higher BE with respect to the same levels from metallic Er [22]. An analogous shift has also been observed in Er_2PdSi_3 and has been attributed to a chemical shift related to the different chemical environment [23]. The Er 4f multiplets of the photoemission spectra are in good agreement with the calculated energy distribution for the Er $4f^{11}$ ground state [21] (see figure 4), confirming the conclusions derived from the XAS spectra. Besides the 4f lines, the difference spectrum shows further spectral weight associated with Er states up to E_F. The VB spectrum of $Er_5Ir_4Si_{10}$ recorded with $h\nu = 47.5$ eV (figure 6) exhibits two broad structures, at around 2.5 and 0.5 eV, separated by shallow minima at 1.2 and 3.4 eV. Two structures at 2.5 and 0.4–0.8 eV separated by shallow minima at 1.15 and 3.15 eV are also present in the $ErSi_{1.7}$VB acquired with $h\nu = 40.8$ eV [24, 25]. In $ErSi_{1.7}$, these structures have been associated to Er 5d

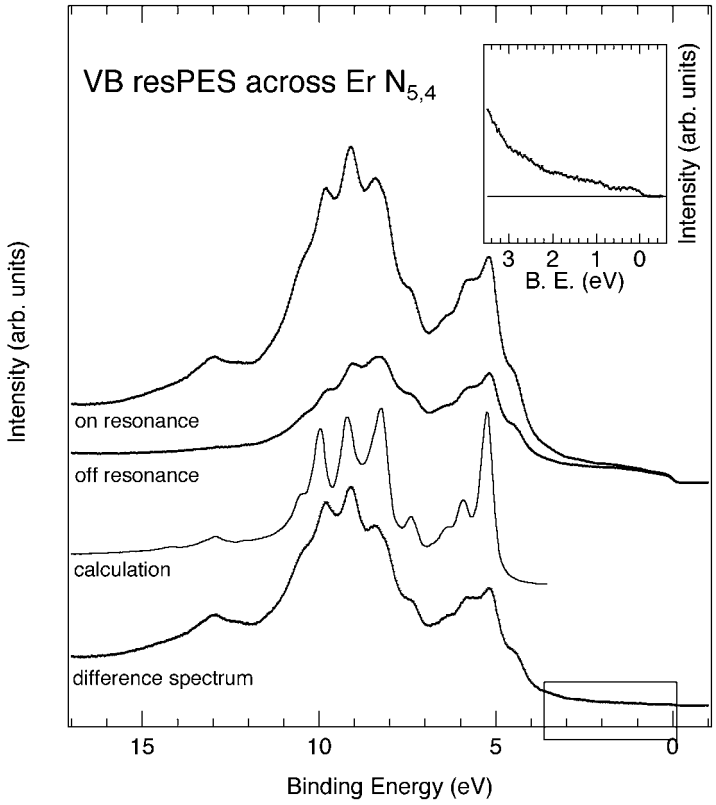

Figure 4. The VB spectra normalized to the photon flux measured across the Er N_{54} absorption edge, on resonance at 167.8 eV and off resonance at 159.8 eV at 115 K.

and Er 5d–Si 3p hybridized states, respectively, from the comparison with the calculated partial DOS of $ErSi_2$ [24, 25]. The analogy of the position of these structures with those in $Er_5Ir_4Si_{10}$ suggests an analogous assignment. In particular, the broad structure at 2.6 eV is associated with Er 5d6p–Si 3p hybridized states. These states are also probably mixed with Ir 5d states, which are usually located in a large band centred around 2 eV, as in Ir single crystal [26]. The contribution of Er states to this 2.6 eV VB structure is supported by the Er 4d $\rightarrow$ 4f resPES, which reveals the presence of Er states in the BE region between 2 and 3 eV (figure 4).

Figure 5 shows the effect of surface degradation on VB spectra measured at $h\nu = 178.5$ eV at a base pressure of 3×10^{-10} mbar. The two spectra have been normalized to the photon flux. We observed a relatively fast degradation of the crystal surface, as seen from a gradual intensity decrease of the Ir 4f core levels (not shown here) as well as a broadening of the Er 4f levels due to the growth of a component with a BE of around 6–7 eV, as seen in figure 5. After some hours, a depletion of the states close to E_F and the growth of a SiO_x component in the Si 2p core level spectrum (not shown here) is observed. The depletion of the states close to E_F was also observed in Er metal, together with the growth of components at 3.8 eV, at 6.1 eV BE associated with H chemisorption, and at 6 eV BE associated with O 2p states [25].

A comparison of the $Er_5Ir_4Si_{10}$ and $Lu_5Ir_4Si_{10}$ VBs is shown in figure 6. The spectra have been measured at the same photon energy ($h\nu = 47.5$ eV) and temperature (RT), above T_{CDW} for both compounds. Both VBs exhibit two broad structures. The cross section of these

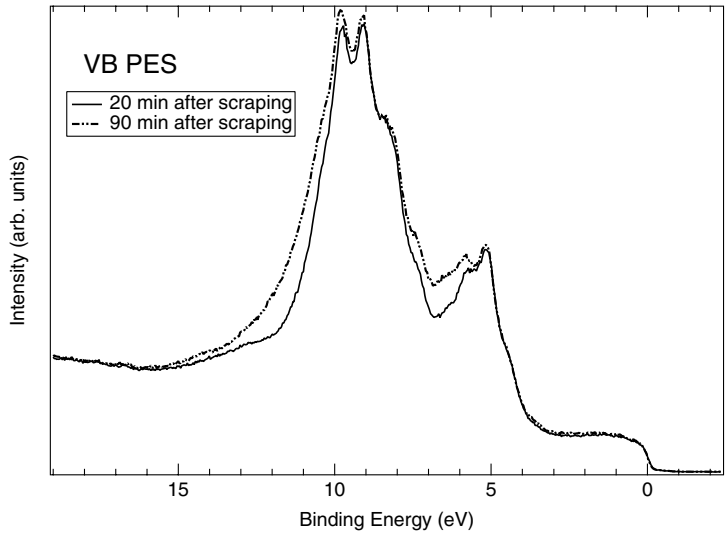

Figure 5. The effect of surface degradation on VB spectra measured at $h\nu = 178.5$ eV at a base pressure of 3×10^{-10} mbar.

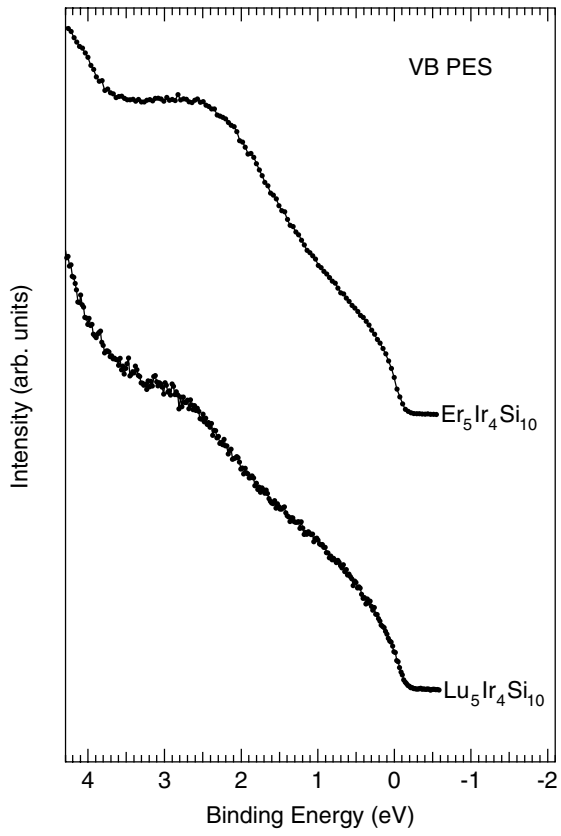

Figure 6. A comparison of the $Er_5Ir_4Si_{10}$ and $Lu_5Ir_4Si_{10}$ VB acquired at the same photon energy ($h\nu = 47.5$ eV) and temperature ($T = 300$ K).

structures is strongly enhanced at $h\nu = 47.5$ eV with respect to higher photon energies, where 4f emission dominates. For $Er_5Ir_4Si_{10}$, these VB structures are located at BEs of around 0.5 and 2.6 eV. For $Lu_5Ir_4Si_{10}$, the latter structure is slightly shifted to a lower BE of around 2.9 eV.

It is also interesting to observe that the main differences between $Er_5Ir_4Si_{10}$ and $Lu_5Ir_4Si_{10}$ VB spectra at $h\nu = 47.5$ eV are found at around 2.6 eV (see figure 6), thus the largest contribution to this structure is probably given by Er states.

The VB BE region between E_F and 1.2 eV acquired at $h\nu = 47.5$ eV for two $R_5Ir_4Si_{10}$ compounds with different R (R = Lu or Er) instead shows a close similarity, which suggests that the states in this region and, in particular, the structure at around 0.5 eV may originate mainly from a covalent mixture of Ir 5d and Si 3sp states. However, in $Er_5Ir_4Si_{10}$, Er N_5 resPES shows the resonant enhancement of a structure centred at about 0.2 eV (figure 4). This structure can be assigned to Er 5d states, in analogy with Er metal, and for the Er 5d character found in this energy region close to E_F in the DOS calculations for $ErSi_2$ [24]. Finally, the shoulder at around 4.5 eV appearing in the Er N_5 resPES spectrum (figure 4) appears to be related neither to the $4f^{11}$ multiplets from the comparison with the theoretical predictions nor to contamination. Since this peak shows a resonant enhancement in Er N_5 resPES, we can argue that it is related to Er states, but an assignment is not straightforward. Considering the DOS calculations for $ErSi_2$ [24] and the previous assignment of the VB states, this structure should correspond to Er 6s and Er 6p states.

The presence of a finite density of Er itinerant states in the VB could explain the differences observed in the Er 4d core level (figure 2) between systems where Er is fully ionized, as in the Er oxides (Er_2O_3 and $Er_2Si_2O_7$) [20], and systems where Er itinerant states are present in the VB, as in metallic Er, in Er_3Rh [18] and in the present system.

No clear reduction in spectral weight at around E_F, correlated with the transition to the CDW state, is observed in the present angle-integrated measurements. In particular, no variation in the Er DOS is observed in the resPES measurements. The CDW phase of $Er_5Ir_4Si_{10}$ is still metallic, since the photoemission spectra show a clear Fermi edge even below the CDW transition. This can be due to the averaging on the three a, b, c directions, while only the Er chains along the c axis, where the periodic lattice distortion caused by the CDW occurs, undergo the metal-to-insulator transition. Indeed, $\rho(T)$ along the a axis exhibits a metallic behaviour even in the CDW state, indicating that the energy gap is not completely opened, i.e. there is a definite electronic density of states within the gap [4]. Since the nesting of the Fermi surface is expected to occur preferentially along the Γ–Z direction of the first Brillouin zone (corresponding to the direction of the c axis of the crystal), an angle-resolved high-resolution photoemission investigation as a function of temperature along this particular direction of the Brillouin zone should show the effects of the CDW formation.

The presence of a finite density of itinerant states in the VB below the CDW transition supports the view that the local-moment magnetism of this system is due to an indirect exchange between the localized 4f electrons mediated by the itinerant conduction electrons. The measurements indicate that, besides the itinerant Si 3sp and Ir 3spd states, itinerant Er states are also present in the VB. In particular, a weak structure associated with Er 5d states that appears close to E_F may play an important role in this exchange coupling.

4. Conclusions

PES, resPES and XAS measurements have been performed on $Er_5Ir_4Si_{10}$ and $Lu_5Ir_4Si_{10}$ single crystals in order to investigate the electronic properties of $Er_5Ir_4Si_{10}$ across the incommensurate CDW transition at 155 K. The measurements indicate that all Er ions have an occupancy of 11 electrons in the 4f shell both above and below the incommensurate CDW transition, supporting the conclusions of previous magnetic measurements [4, 7].

The character of the VB states has been investigated by resPES. In particular, the off-resonance spectra have been subtracted from the spectra obtained on-resonance on the multiplet

lines appearing in the Er N_{54} and M_5 XAS. In the difference spectra, the contribution from the Er partial DOS in the VB is highlighted. Both above and below T_{CDW}, the difference spectra show a weak spectral weight associated with Er states between E_F and the Er 4f multiplets. The presence of itinerant Er non-f states in the VB is supported by the lineshape of the Er 4d core level.

The similarity of the VB spectra of $Er_5Ir_4Si_{10}$ and $Lu_5Ir_4Si_{10}$ suggests that the structure at around 0.5 eV that is present in both samples may originate from a covalent mixture of Ir and Si sp states. The structure at a BE of around 2.6 eV is assigned to Er–Si hybridized states for the analogy with the $ErSi_{1.7}$ VB. Er N_{54} resPES reveal a structure originating from Er states centred at a BE of 0.2 eV which is assigned to Er 5d states. From the present angle-integrated photoemission measurements, the system appears metallic both above and below the incommensurate CDW transition with no clear variation of the Er DOS.

Acknowledgments

Work at the BACH beamline was supported by the FIRB (Investment Fund for Basic Research) project No RBNE0155X7. JAM is supported by the A von Humboldt Foundation.

References

[1] Braun H F, Yvon K and Braun R H 1980 *Acta Crystallogr.* B **36** 2397
[2] Yang H D, Klavins P and Shelton R N 1991 *Phys. Rev.* B **43** 7688
[3] Galli F, Ramakrishnan S, Taniguchi T, Nieuwenhuys G J, Mydosh J A, Geupel S, Ludecke J and van Smaalen S 2000 *Phys. Rev. Lett.* **85** 158
[4] Jung M H, Kim H C, Migliori A, Galli F and Mydosh J A 2003 *Phys. Rev.* B **68** 132102
[5] van Smaalen S, Shaz M, Palatinus L, Daniels P, Galli F, Nieuwenhuys G J and Mydosh J A 2004 *Phys. Rev.* B **69** 014103
[6] Becker B, Patil N G, Ramakrishnan S, Menovsky A A, Nieuwenhuys G J and Mydosh J A 1999 *Phys. Rev.* B **59** 7266
[7] Galli F, Feyerherm R, Hendrikx R W A, Ramakrishnan S, Nieuwenhuys G J and Mydosh J A 2000 *Phys. Rev.* B **62** 13840
[8] Shelton R N, Hausermann-Berg L S, Klavins P, Yang H D, Anderson M S and Swenson C A 1986 *Phys. Rev.* B **34** 4590
[9] Yang H D, Shelton R N and Braun H F 1986 *Phys. Rev.* B **33** 5062
[10] Mydosh J A 1993 *Spin Glasses: an Experimental Introduction* (London: Taylor and Francis)
[11] Galli F, Nieuwenhuys G J, MacLaughlin D E, Heffner R H, Amato A, Bernal O O and Mydosh J A 2002 *Physica* B **319** 282
[12] van der Marel D 2006 private communication
[13] Zangrando M, Finazzi M, Paolucci G, Comelli G, Diviacco B, Walker R P, Cocco D and Parmigiani F 2001 *Rev. Sci. Instrum.* **72** 1313
[14] Zangrando M, Zacchigna M, Finazzi M, Cocco D, Rochow R and Parmigiani F 2004 *Rev. Sci. Instrum.* **75** 31
[15] Thole T, Carra P, Sette F and van der Laan G 1992 *Phys. Rev. Lett.* **68** 1943
[16] Ogasawara H and Kotani A 2001 *J. Synchrotron Radiat.* **8** 220
[17] Ogasawara H, Kotani A and Thole B T 1994 *Phys. Rev.* B **50** 12332
[18] Talik E, Neumann M, Kusz J, Bohm H, Mydlarz T, Heimann J and Winiarski A 1998 *J. Magn. Magn. Mater.* **186** 33
[19] Guerfi N, Tan T, Veuillen J Y and Lollman D B 1992 *Appl. Surf. Sci.* **56** 501
[20] Hafidi K, Ijdiyaou Y, Azizan M, Ameziane E L, Outzourhit A and Brunel M 1997 *Appl. Surf. Sci.* **108** 251
[21] Gerken F 1983 *J. Phys. F: Met. Phys.* **13** 703
[22] Lang J K, Baer Y and Cox P A 1981 *J. Phys. F: Met. Phys.* **11** 121
[23] Szytula A, Jazierski A and Penc B 2003 *Physica* B **327** 171
[24] Magaud L, Veuillen J Y, Lollman D, Nguyen Tan T A, Papaconstantopoulos D A and Mehl M J 1992 *Phys. Rev.* B **46** 1299
[25] Wetzel P, Haderbache L, Pirri C, Peruchetti J C, Bolmont D and Gewinner G 1991 *Phys. Rev.* B **43** 6620
[26] Klebanoff L E and van Campen D G 1992 *Phys. Rev.* B **46** 9744